Available online at www.sciencedirect.com
ScienceDirect
Coastal Engineering 55 (2008) 375–390
Coastal Engineering
An International Journal for Coastal, Harbour and Offshore Engineers
www.elsevier.com/locate/coastaleng

Statistical simulation of wave climate and extreme beach erosion

D.P. Callaghan [a,*], P. Nielsen [a], A. Short [b], R. Ranasinghe [c]

[a] Division of Civil Engineering, The University of Queensland, Brisbane, 4072, Australia
[b] Coastal Studies Unit, School of Geosciences, University of Sydney, Sydney NSW 2006, Australia
[c] Department of Natural Resources, New South Wales, GPO Box 39, Sydney, NSW 2001, Australia

Received 11 May 2007; received in revised form 18 December 2007; accepted 18 December 2007
Available online 19 February 2008

Abstract

Recent developments in extreme values modelling have been used to develop a framework for determining the coastal erosion hazard on sandy coastlines. This framework quantitatively reproduced the extreme beach erosion volumes obtained from field measurements at Narrabeen Beach, Australia. This encouraging finding was achieved using Kriebel and Dean's [Kriebel, D.L. and Dean, R.G., 1993. Convolution method for time-dependent beach profile response. Journal of Waterway, Port, Coastal and Ocean Engineering, 119(2): 204–226.] simple beach erosion and accretion model. The method includes allowances for joint probability between all basic erosion variates including; wave height, period and direction, event duration, tidal anomalies and event spacing. A new formulation for the dependency between wave height and period has been developed. It includes the physical wave steepness limitation. Event grouping, where significantly more erosion can occur from two closely spaced storms is handled by temporally simulating the synthetic wave climate and the resulting beach erosion and accretion.

Keywords: Joint probability; Statistics; Monte Carlo simulation; Equilibrium profiles; Beach erosion

1. Introduction

Coastal zone managers are increasingly seeking accurate quantitative predictions of beach erosion hazards within a probabilistic framework. This avoids the ad hoc approach in which a benchmark event (usually the largest measured historical event) is applied to assess beach erosion and inundation. This benchmark approach provides limited information regarding the return period of the predictions and excludes confidence limit estimation. For systems involving two or more random variables, the return period of outcomes is not equal to the forcing return period of a particular variate (Hawkes et al., 2002). For example, a 100-year wave height historical event does not necessarily result in a 100-year beach erosion. One reason for this, among others, is the dependency of erosion volumes on storm duration. Kriebel and Dean (1993) showed that during erosion events, there was a finite time required for the new equilibrium profile to form. Consequently, shorter duration events having the same peak wave height result in less beach erosion.

Another problem in applying a benchmark event is that it excludes the merging of independent meteorological events into one beach erosion event. For example, two events, of equal magnitude occurring within a few days generate more erosion than if separated by many months, in which the beach is able to recover from the first erosion event.

This paper presents and applies a new and comprehensive method to determine the beach erosion hazard using recently developed statistical methods. The predictions are compared to extreme statistics of beach erosion volume measured at Narrabeen Beach to evaluate the method's potential for further investigation and application to other locations.

Four alternative parametric methods are available to replace the benchmark approach. They are; fitting distributions directly to erosion measurements; the structural variable method (SVM); joint probability method by integration and full temporal simulation. This study reviews these statistical methods for estimating extreme quantities and applies a

* Corresponding author. Tel.: +61 7 3365 3914; fax: +61 7 3365 4599.
E-mail addresses: Dave.Callaghan@uq.edu.au (D.P. Callaghan), P.Nielsen@uq.edu.au (P. Nielsen), A.Short@geosci.usyd.edu.au (A. Short), Rosh.Ranasinghe@dnr.nsw.gov.au (R. Ranasinghe).

0378-3839/$ - see front matter © 2007 Elsevier B.V. All rights reserved.
doi:10.1016/j.coastaleng.2007.12.003

combination of statistical and physical mechanisms to refine the full temporal simulation approach. This refined method is shown to perform well when compared against field measurements.

The paper is arranged as follows. Section 2 provides an overview of statistical methods available and justifies our selection between these approaches. The individual statistical distributions of the adopted framework are demonstrated in Section 3. The structural function is also discussed in Section 3. Field measurements obtained from Narrabeen Beach over *ca* 30 years are analysed in Section 4 to determined empirical estimates of extreme beach erosion. Section 5 compares the proposed method with the field measurements. Conclusions and future directions are given in Sections 6 and 7 respectively.

2. Review of methods

This section reviews four statistical methods for determining extreme value beach erosion. These methods could equally be applied to beach inundation or other coastal hazards.

2.1. Fitting distributions directly to measurements

Fitting distributions directly to erosion measurements requires many decades of continuous bathymetric measurements that are generally not available. This method also does not allow future changes of model variates to be incorporated in the extreme values prediction (e.g., climate change). Narrabeen and Moruya beaches are the only two locations in Australia where this method could be applied.

Narrabeen and Moruya Beaches unique cases in Australia and most likely the entire world, where continuous beach profile records exist. These measurements facilitate estimation of the beach erosion probability scale. There are many sites around the world that do have profile measurements for major storms. However, there is no reliable method to estimate event probabilities when the measurements do not contain the small to mid range erosion events that are required to overcome sampling error in the statistical analysis.

2.2. Structural variable method (SVM)

The structural variable method takes the measured wave parameters and water levels and uses a structural function to determine the quantity of interest. The structural function could predict quantities such as beach erosion amount, flooding extent and seawall overtopping flow rate. For example, the beach erosion structural function would involve the following calculations for each measured storm;

1. wave transformation from offshore to nearshore (e.g., using a spectral wave model);
2. estimation of nearshore sediment transport (e.g., using a cross-shore profile model); and
3. evaluating the change in the profile (e.g., volume of sand loss above mean sea level).

(In this example, additional field information is required to enable calibration and validation of the profile model.) Having obtained the erosion volume for each measured storm, the next step in the SVM is to sort the erosion volumes in ascending order and assign empirical probabilities. These computed estimates are then extrapolated using a fitted extreme value distribution, which implicitly excludes information within the structural function above the measurement range. Another weakness of this approach is that temporal changes are limited to the measurement period. Nevertheless, Garrity et al. (2006) demonstrates that this method is capable of yielding satisfactory agreement with other methods for estimating coastal flooding hazards.

2.3. Joint probability method (JPM)

The joint probability method applies various statistical modelling techniques to all quantities required by the structural function, including any dependency between variates. These models are formulated into a single joint probability density function, which is integrated over all combinations of variate ranges that exceed a particular threshold to determine the exceedance probability. Hence, information from the structural function above the measurements is included.

This method excludes temporal variations (e.g., sea-level rise or La Niña/El Niño) and the processes where independent events are merged into a single event. This very situation occurs at Narrabeen Beach in June 2007 where several independent (generated by different meteorological features) wave storm events that occurred in quick succession produce significant beach erosion. At Narrabeen, these events, in isolation, would not produce significant beach erosion. However, as there was limited time for beach recovery, subsequent events merely pick up from where the previous event left off. Consequently, excluding event merging is a significant limitation at Narrabeen Beach (and most likely other beaches nearby).

On a more practical note, it is very difficult, and often impossible, to determine the variate space that yields an outcome quantity that exceeds a particular threshold. For example, beach erosion is dependent on both the present storm parameters and antecedent beach conditions. Antecedent beach condition is very hard to describe in terms of just one or two parameters and is not typically measured like wave parameters and water levels. Hence, it is usually unavailable for inclusion into the joint probability density function. Consequently, it is impossible to determine the parameter space required to exceed a particular beach erosion volume.

2.4. Full temporal simulation

The full temporal simulation method involves three phases; event simulation to generate a synthetic climate record of wave parameters and water levels; the computing of desired quantities using this synthetic record from various structural functions; and the computing of return levels of the desired quantities. A recent example of this method for coastal flooding hazard is provided by Garrity et al. (2006).

With an appropriate Poisson process model for the time between consecutive events, this approach can handle event grouping and has the potential to include climate change and non-stationary processes (La Niña/El Niño).

This method does not, however, perform well on non-linear structural functions (e.g., Hawkes, 2000). In some cases, the final result does not follow the usual extreme value distributions. This is irrelevant when return levels are easily and empirically determined. However, empirical methods are incapable of providing good extrapolation if future temporal variations are to be included. This limitation is avoided if future changes are not included by using long simulation lengths to improve the empirical estimates at large return periods. However, if climate change/variability processes are included, their time scales define the simulation length and consequently, limit the return period that can be confidently estimated. Bootstrapping techniques can be used to estimate the uncertainty introduced purely by limiting the Monte Carlo simulation length.

This approach was adopted for the coastal erosion hazard determination given that the full temporal simulation method is capable of including event grouping and that it overcomes the non-linearity issue of post fitting extreme values distribution. The full temporal simulation is implemented using the following eight steps:

1. Identify meteorologically independent storm events.
2. Fit extreme value distributions to wave height and storm duration (marginal distributions).
3. Fit the dependency distribution between wave height and storm duration.
4. Fit the wave period and peak tidal anomaly conditional distributions.
5. Determine the empirical distribution for wave direction.
6. Fit a non-homogenous Poisson distribution to the spacing between storms.
7. Simulate the wave climate using the fitted distributions including storm spacing.
8. Estimate extreme values of beach erosion from the simulated wave climate.

Steps 1–5 were proposed by Hawkes et al. (2002) and steps 6–8 allow the inclusion of storm grouping and non-stationary processes to be included. This approach is different from others in that steps 4, 6, 7 and 8 are new.

The long period of continuous wave measurements required for this method are readily obtainable at most sites around the world from either direct measurements or wave hindcasting. Consequently, this method can be applied at different sites after minor adjustments are made to both the joint probability distribution and structural function to ensure the approach is suitable for the particular location. For example, if these methods are applied to beaches protected by the Great Barrier Reef which are typically only exposed to sea, the wave period could be determined using a fixed wave steepness (Hawkes et al., 2002). Where as, on an open coast that is exposed to both sea and swell waves, a statistical description of the wave period is required.

3. Hazard estimation

In this section, the adopted statistical framework (Section 3.1) and the structural function (Section 3.2) are applied to estimate the storm erosion hazard at Narrabeen Beach, Sydney, Australia (see Fig. 1a and c).

3.1. Synthetic climate modelling

The offshore wave measurements were obtained from Botany Bay (Lawson and Abernethy, 1975; Trindade et al., 1993; Youll, 1981) and Long Reef (Kulmar et al., 2005), both located near Sydney (see Fig. 1b). The non-directional Botany Bay wave

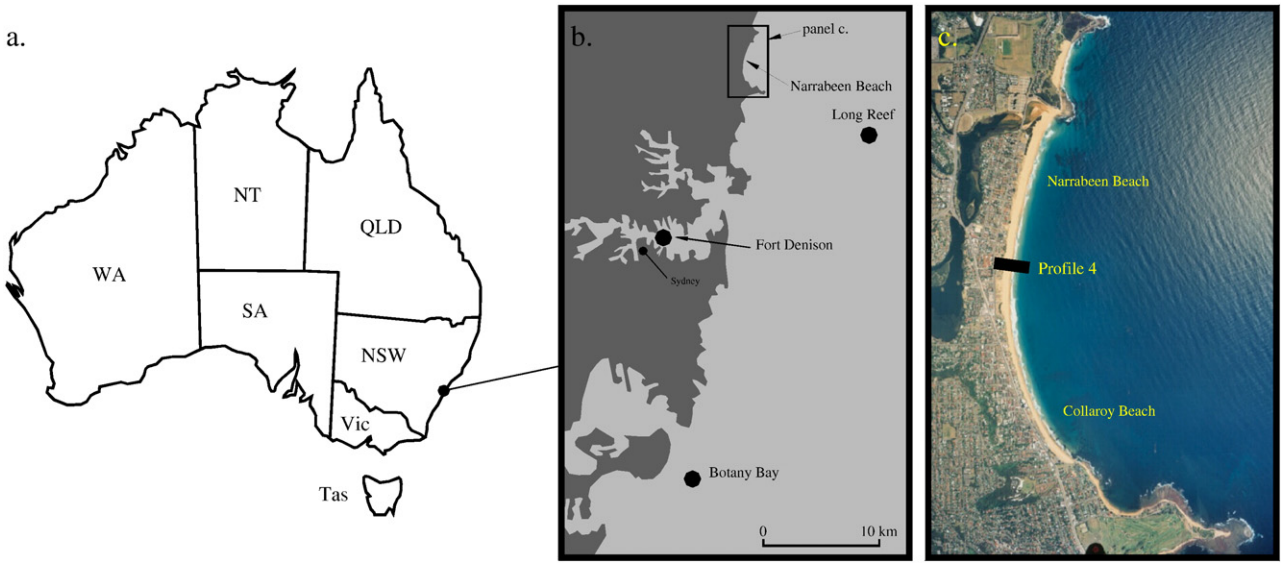

Fig. 1. Locality map for field measurements. a. Location of Sydney within Australia; b. The Botany Bay and Long Reef wave buoy locations and the Fort Denison tidal recording station; and c. The location of long term beach profile surveys at Narrabeen Beach (profile 4) (Short and Trembanis, 2004).

buoy is located at approximately E**33**8770 m; N6**23**1900 m (GDA Zone 56, ICSM, 2002) and the measurements used in this article extend from 8 April 1971 to 22 May 2006 or *ca* 35 years. The Long Reef wave buoy has been located at 13 positions that are within 2 km of E**35**3492 m; N6**26**1660 m. Long Reef measurements for directional wave statistics cover the period extending from March 1992 through to March 2006, a sample length of 14 years with 83% of this period captured (Kulmar et al., 2005). Both buoys are located in approximately 80 m water depth. The tidal level measurements, that exclude wave set-up and run-up, were measured at Fort Denison (Anonymous, 1995) and extend from June 1914 through to December 2005, or *ca* 92 years (see Fig. 1b).

3.1.1. Step 1—identify meteorologically independent storm events

For the purpose of this study, storm events were identified as periods where significant offshore wave height (H_s) exceeded 3 m (Kulmar et al., 2005; Lord and Kulmar, 2000). These periods were then manually assessed (accepted with or without adjustment or rejected) to ensure that each wave event represents one meteorological system. Fig. 2 shows the definition used for storm duration and peak wave height.

3.1.2. Step 2—fit extreme value distributions to wave height and storm duration (marginal distributions)

The extreme value analysis has, historically, involved selecting from three limiting extreme values distribution families; Gumbel (Type I), Fréchet (Type II) and Weibull (Type III). For examples of different fitting methods used to apply these distributions, see Goda (1988), Mathiesen et al. (1994), Alves and Young (2003) and Dawson (2000). These three families provide different tail behaviour as follows; at the extreme limit, Weibull has a finite asymptotic value while both Gumbel and Fréchet are unbounded; and the approach to unity in the tail of $F(x)$ (=Pr$\{X \leq x\}$) varies greatly between the three families. This leads to qualitative and quantitative differences between extreme values prediction. Hence, the adopted distribution is a subjective judgment by the modeller and not directly determined from the measurements. Coles (2001) points out that inferences such as confidence limits are also limited to the adopted family and hence do not include the uncertainty associated with the family selection. Consequently, once the family type is chosen, the confidence limits are reduced as uncertainty has been artificially removed. Hence, we follow the method of Hawkes et al. (2002), in which the distribution selection is included in the statistical modelling by using the generalised Pareto (GP) distribution (which is the combination of three statistical families). The GP distribution is given by

$$\Pr\{X>x|X>u\} = \begin{cases} \left\{1+\xi\sigma^{-1}(x-u)\right\}^{-1/\xi} & \xi \neq 0 \\ e^{-\frac{x-u}{\sigma}} & \xi = 0 \end{cases} \quad (1)$$

with σ and ξ being the GP scale and shape parameters (Coles, 2001) and u being the threshold that ensures model convergence. The parameters are estimated using the maximum likelihood method, which maximises the probability of the data given the model, i.e.,

$$\begin{aligned} \Pr\{\mathbf{x}|\sigma,\xi\} &= \Pr\{X_1 = x_1|X_1>u\} \times \Pr\{X_2 = x_2|X_1>u\} \times \ldots \times \Pr\{X_N = x_N|X_N>u\} \\ &= \prod_{i=1}^{N} \Pr\{X_i = x_i|X_i>u\} \\ &= \prod_{i=1}^{N} f(x_i) \end{aligned} \quad (2)$$

where $f(x) = \frac{dF(x)}{dx} = \frac{d}{dx}[1 - \Pr\{X>x|X>u\}]$, N is the number of measurements, $f(x)$ and $F(x)$ being the probability density and distribution functions respectively and $\mathbf{x}$ is the vector of measurements. For numerical reasons (finite floating point range) it is more convenient to maximise the logarithm of Eq. (2), i.e.,

$$\begin{aligned} \ell(\mathbf{x}|\sigma,\xi) &= \sum_{i=1}^{N} \ln f(x_i) \\ &= \begin{cases} -N\ln\sigma - \left(1+\xi^{-1}\right)\sum_{i=1}^{N} \ln\left\{1+\xi\sigma^{-1}(x_i-u)\right\} & \xi \neq 0 \\ -N\ln\sigma - \sigma^{-1}\sum_{i=1}^{N}(x_i-u) & \xi = 0 \end{cases} \end{aligned} \quad (3)$$

and we use the multi-dimensional downhill simplex method (Nelder and Mead, 1965) to maximise Eq. (3) by minimising $-\ell(\mathbf{x}|\sigma,\xi)$.

Other parameter estimators (moments, L-moments, Bayesian and least squares regression) were discounted based on Hawkes (2000) and Coles (2001) recommendations and the recently provided examples from Méndez et al. (2006), Coles (2004), Coles and Pericchi (2003), Dawson (2000), Bruun and Tawn (1998) and Morton et al. (1997). However, Kamphuis (2000) quite rightly points out that the literature does not indicate a preferred method to estimate distribution parameters. The proposed statistical framework; however, can be completed with any parameter estimator or even a mixture of estimators. Davidson and MacKinnon (2004) provide an extensive description of various parameter estimators. The Bayesian method, where parameter distributions are estimated, does not lend itself to structural functions that allow statistically independent events to merge. Nevertheless, the interested reader is referred to Beirlant et al. (2004), Behrens et al. (2004) and Coles and Tawn (2005) for Bayesian techniques.

For the maximum significant wave height during a storm ($H_{s,max}$ on Fig. 2) at Botany Bay, the GP distribution converges for

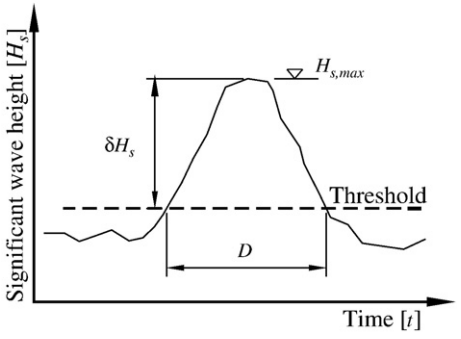

Fig. 2. Definition sketch for storm duration.

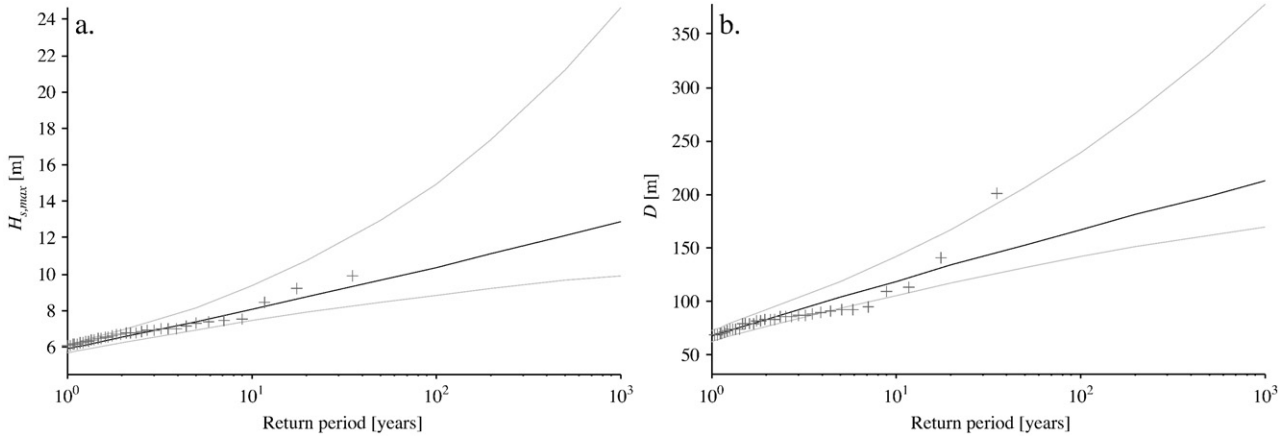

Fig. 3. The return level plot for a. $H_{s,max}$ and b. D at the Botany Bay wave buoy using the GP distribution. Black line is the fitted model; gray lines are the 95% confidence limits; and + are the empirical estimations.

u=4.5 m with σ and ξ being 0.86 m [0.68 m; 1.08 m] and 0.03 [−0.11; 0.24] respectively with 95% confidence ranges provided in the square brackets. The 95% confidence range for the shape parameter ξ indicates that the underlying distribution, in the GEV parametric approach, is well approximated by the Gumbel, Fréchet or Weibull distributions. Hence, the uncertainty would have been underestimated (reflected in the confidence range) had the distribution shape been selected a priori. The storm duration (D on Fig. 2) GP distribution converges for u=40 h, σ=24 h [19; 30] and ξ=−0.03 [−0.11; −0.24]. Fig. 3a and b shows the fitted distribution return level plots with 95% confidence limits and the Botany Bay empirical estimates using $\Pr\{x_i\}=i/(N+1)$, where $x_1 \le x_2 \le x_3 \ldots \le x_N$.

3.1.3. Step 3—fit the dependency distribution between wave height and storm duration

The logistics model (Tawn, 1988),

$$\Pr\{X \le x, Y \le y\} = F(x,y) = e^{-\left[x^{-\alpha^{-1}}+y^{-\alpha^{-1}}\right]^{\alpha}} \tag{4}$$

where x and y are the rescaled Fréchet variates and α is the dependent parameter, used for dependency modelling between $H_{s,max}$ and D. When α=1, Eq. (4) reduces to x and y being independent variables and when α=0, Eq. (4) reduces to perfectly dependent variables. The standard Fréchet distribution function is

$$\Pr\{Z \le z\} = F(z) = e^{-1/z}, \quad z > 0. \tag{5}$$

The dependency parameter α was estimated by maximising the log-likelihood,

$$\ell(\mathbf{x},\mathbf{y}|\alpha) = \sum_{i=1}^{N} \begin{cases} \ln \dfrac{\partial^2 F}{\partial x \partial y}\Big|_{x_i,y_i} & \text{if}(x_i,y_i) \in [u'_x,\infty) \times [u'_y,\infty) \\ \ln \dfrac{\partial F}{\partial x}\Big|_{x_i,u'_y} & \text{if}(x_i,y_i) \in [u'_x,\infty) \times \left(-\infty,u'_y\right) \\ \ln \dfrac{\partial F}{\partial y}\Big|_{u'_x,y_i} & \text{if}(x_i,y_i) \in \left(-\infty,u'_x\right) \times [u'_y,\infty) \\ \ln F\left(u'_x,u'_y\right) & \text{if}(x_i,y_i) \in \left(-\infty,u'_x\right) \times \left(-\infty,u'_y\right) \end{cases} \tag{6}$$

where $\mathbf{x}$ and $\mathbf{y}$ are the rescaled Fréchet variate vectors containing x_i and y_i elements, u'_x and u'_y are the thresholds obtained in the marginal distribution fitting and converted to the Fréchet scale. The $H_{s,max}$ and D are transformed to Fréchet variates using

$$\tilde{X} = \begin{cases} -\left[\ln\left\{1-\zeta_u\left[1+\xi\left(\dfrac{X-u}{\sigma}\right)\right]^{\frac{-1}{\xi}}\right\}\right]^{-1} & \xi \neq 0 \\ -\left[\ln\left\{1-\zeta_u \exp\left(-\dfrac{x-u}{\sigma}\right)\right\}\right]^{-1} & \xi = 0 \end{cases} \tag{7}$$

where X is either $H_{s,max}$ or D, $\zeta_u=\Pr\{X<u\}$, and $\tilde{X}$ is the transformed variable whose distributions follow the standard Fréchet for $X>u$. The probability of exceedance for the logistics model is

$$\Pr\{X \ge x, Y \ge y\} = 1 - e^{-x^{-1}} - e^{-y^{-1}} + e^{-(xy)^{-1}\left(x^{\alpha^{-1}}+y^{\alpha^{-1}}\right)^{\alpha}} \tag{8}$$

for $\alpha \neq 0$ and where x and y are Fréchet variates. We determined return level contours using the following method; for the return period, in years, T_{RL}, with N_y events per year; solve for the locus of (x,y) when $\Pr\{X \ge x,\ Y \ge y\}=(T_{RL}N_y)^{-1}$; and transform the Fréchet scale locus to the physical scale using Eq. (7) in reverse. The downhill simplex method was used to maximise Eq. (6) by minimising $-\ell(\mathbf{x},\mathbf{y}|\alpha)$ and yielded α=0.64 [0.58; 0.69]. This result indicates that dependency between $H_{s,max}$ and D does exist as $\alpha<1$ at the upper 95% confidence limit. Fig. 4 illustrates this dependency.

3.1.4. Step 4—fit the wave period and peak tidal anomaly conditional distributions

Both tidal anomaly (R) and significant wave period (T_s) are conditionally related to $H_{s,max}$ for the following physical reasons; tidal anomalies are often produced by the same meteorological feature generating the waves; wave period is governed by physical mechanisms that limits its range (e.g., for

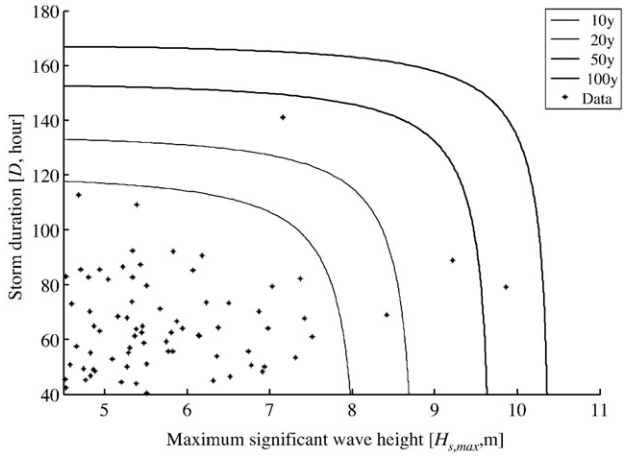

Fig. 4. Logistic exceedance return level contours (return periods, T_{RL}, shown in legend) and measurements (∗) using the generalised Pareto marginal distribution for the $H_{s,max}$ and D from Botany Bay wave buoy.

a stable H_s, wave steepness restricts the possible range that T_s can have). As wave height is typically the dominant variate for beach erosion, it was chosen as the conditional variate.

East coast lows account for *ca* 39% of the wave climate at Sydney (Short and Trenaman, 1992). This type of meteorological event will locally generate waves, provide onshore winds and low atmospheric pressures near the coast, with the last two characteristics able to generate positive tidal anomalies. However, Mid-latitude cyclones account for *ca* 46% of the wave climate. These systems are typically located several thousand kilometres from Sydney and hence do not produce conditions suitable to generate positive tidal anomalies. Consequently, we expect a weak correlation between storm R and $H_{s,max}$.

The logistics model was again used for dependency between R with $H_{s,max}$ and it is assumed that any dependency between storm duration and tidal anomaly is adequately modelled through the wave height dependency. That is, we estimate both D and R given $H_{s,max}$. This is a significant simplification over constructing a trivariate joint distribution (see, for example, Coles and Tawn, 1991; Shi, 1995). The GP distribution for R converged using $u \geq 0.175$ m with $\sigma = 0.06$ m [0.04; 0.07] and $\xi = 0.11$ [−0.04; 0.32] Fitting the logistics model yielded $\alpha = 0.74$ [0.69; 0.8], confirming the expected weak dependency between R and $H_{s,max}$ (Fig. 5).

Comparing Figs. 4 and 5 suggests that R is more dependant on $H_{s,max}$ than D. However, the logistic dependency model parameter α, indicates the opposite. This suggests that one or more of the marginal or dependency distributions is a poor approximation of the measurements. The strongest candidate for this poor approximation is the marginal distribution of D (see Fig. 3b).

The proposed conditional modelling for wave period uses a log-normal distribution

$$\Pr\{T_s = x\} = \left\{(x-\kappa)\sigma\sqrt{2\pi}\right\}^{-1} e^{-\frac{1}{2}\left(\frac{\ln(x-\kappa)-\mu}{\sigma}\right)^2} \tag{9}$$

where model parameters κ, μ and σ are dependent on $H_{s,max}$. The minimum significant wave period (T_s) measured at Botany Bay is $T_{s,min} \approx 3.9\ H_s^{0.5}$ (H_s in metres and $T_{s,min}$ in seconds), which represents the practical maximum storm wave steepness (H_s/L_s) of *ca* 0.04, where L_s is the wavelength from T_s. Consequently, the dependency between distribution parameters and expectation should ensure most random realizations of T_s exceed this limit. To model this, we stipulate the expectation as

$$E(T_s) = \kappa + e^{\mu+\frac{\sigma^2}{2}} \sim k_1 H_s^{k_2} \tag{10}$$

where k_1 and k_2 are constants. Consequently, the suggested dependence on H_s that is similar to Eq. (10) is

$$(\kappa, \mu, \sigma) = \left(aH_s^b, \ln cH_s^d, \sqrt{2\ln fH_s^g}\right) \tag{11}$$

yielding the expectation

$$E(T_s) = aH_s^b + cfH_s^{d+g}. \tag{12}$$

The log-likelihood of Eq. (9) is

$$\ell(\mathbf{x}|\kappa,\mu,\sigma) = -N\left(\ln\left(\sigma\sqrt{2\pi}\right) + \frac{\mu^2}{2\sigma^2}\right) + \left(\frac{\mu}{\sigma^2} - 1\right) \times \sum_{i=1}^{N} \ln(\mathbf{x}_i - \kappa) - \frac{1}{2\sigma^2}\sum_{i=1}^{N}\left[\ln(\mathbf{x}_i - \kappa)\right]^2 \tag{13}$$

where $\mathbf{x}$ is the vector of measurements. Substituting Eq. (11) into this log-likelihood yields

$$\ell(\mathbf{x}|a,b,c,d,f,g) = -N\left(\ln\left(2\sqrt{\pi\ln fH_s^g}\right) + \frac{\left(\ln cH_s^d\right)^2}{4\ln fH_s^g}\right) + \left(\frac{\ln cH_s^d}{2\ln fH_s^g} - 1\right)\sum_{i=1}^{N}\ln\left(\mathbf{x}_i - aH_s^b\right) - \frac{1}{4\ln fH_s^g}\sum_{i=1}^{N}\left[\ln\left(\mathbf{x}_i - aH_s^b\right)\right]^2. \tag{14}$$

Table 1 provides the model parameters estimated for the Botany Bay wave buoy by maximising Eq. (14) using Lasdon

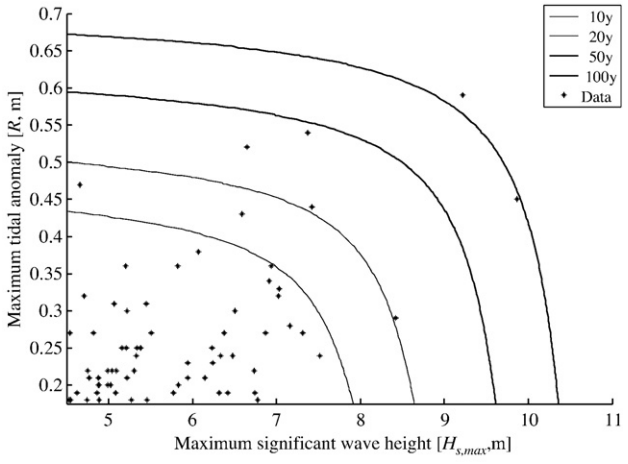

Fig. 5. Logistic exceedance return level contours (return periods, T_{RL}, shown in legend) and measurements (∗) using the generalised Pareto marginal distribution for the $H_{s,max}$ and R from Botany Bay wave buoy and Fort Denison respectively.

Table 1
Wave period model parameters determined from maximising Eq. (14) for the Botany Bay wave buoy when H_s and T_s are in metres and seconds respectively

Model parameter	Estimation	Lower 95% confidence limit	Upper 95% confidence limit
a	3.005	3.001	3.01
b	0.543	0.542	0.544
c	4.82	4.8	4.84
d	−0.332	−0.335	−0.329
f	1.122	1.121	1.123
g	−0.039	−0.04	−0.038

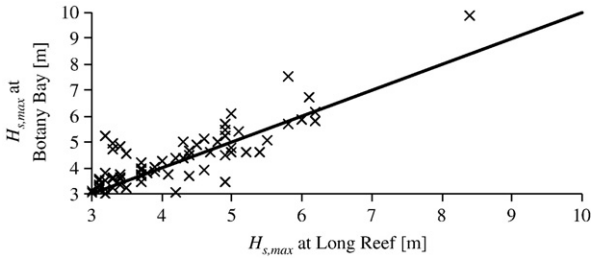

Fig. 7. Measured peak storm $H_{s,max}$ (×) for Botany Bay and Long Reef wave buoys for all simultaneously events. The solid continuous line corresponds to identical $H_{s,max}$ at the two stations.

et al. (1978) when H_s and T_s are in metres and seconds respectively. Fig. 6 shows the wave measurements, the conditional probability model and $T_{s,min}$, with the model reasonably reproducing the lower limit on wave period.

3.1.5. Step 5—determine the empirical distribution for wave direction

The wave direction is not measured by the Botany Bay wave buoy. The nearby Long Reef wave buoy provides wave directions, albeit over a shorter interval. Both buoys are located in similar water depth and at these depths, bathymetry contours are reasonably parallel. Fig. 7 shows $H_{s,max}$ during the overlapping period, indicating that similar but not exactly equal conditions are measured, with the linear relationship of $H_{s,max,Botany\ Bay} = 1.04\ H_{s,max,Long\ Reef}$ explaining *ca* 70% of the variance. Consequently, it is reasonable to use Long Reef measurements of $H_{s,max}$ and peak spectral wave direction (θ_p, measured clockwise from true North, see right panel of Fig. 8) to determine the empirical wave direction distribution.

The left panel of Fig. 8 shows the peak spectral wave direction, θ_p, at Long Reef with direction clustering around $\theta_p \sim 175°$. There also appears to be a tendency that extreme events occur at $\theta_p \in [150°; 170°]$. The measurements also illustrate a reversed log-normal shape for $H_s \in [3\ m; 4\ m]$ (not shown). However, fitting a reversed log-normal distribution yielded poor quantitative agreement with the measurements. Finally, the test for statistically significant dependency between $H_{s,max}$ and θ_p failed and hence, θ_p was assumed independent of $H_{s,max}$. An empirical cumulative probability model following the measurements was adopted as illustrated in Fig. 9.

3.1.6. Step 6—fit a non-homogenous Poisson distribution to the spacing between storms

This step models the duration between consecutive storms. This is of particular interest as it is likely that two storm events occurring within a few days of each other may yield more extensive beach erosion than a single event. Further, characterising the seasonal changes in event frequency from the different meteorological processes generating the waves (Short and Trenaman, 1992) is also essential for a physically plausible Monte Carlo simulation.

Fig. 10 shows the measured seasonal variation in storm occurrences, with winter receiving more events than summer. The seasonal variation in storm occurrence, while ignoring storm grouping, was modelled using a non-homogeneous Poisson process. Initially, we followed the usual method in which the storm duration is considered small compared to the spacing between events as typically applied in the literature (see, for example, Coles, 2001; Davison and Smith, 1990; Luceño et al., 2006). However, when fitting the Poisson process to the time between event occurrence (i.e., time from the start of consecutive events), there was a systematic deviation at quantile levels below

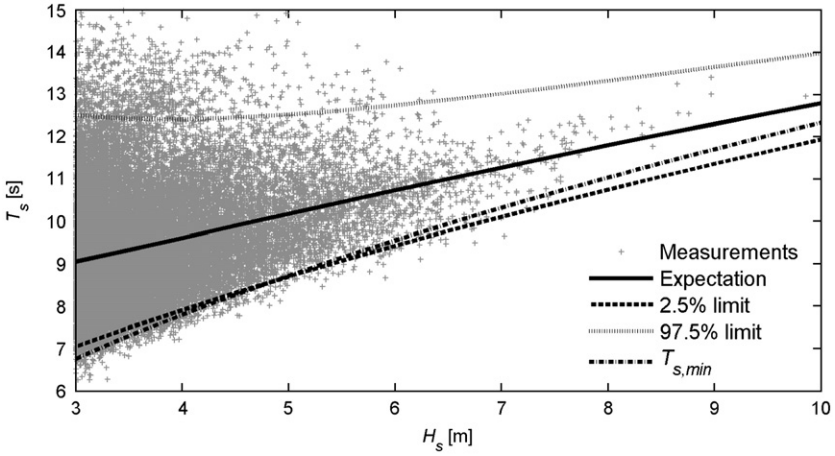

Fig. 6. Measured T_s and H_s (+) at Botany Bay where $H_s > 3$ m, the T_s expectation (—), the 2.5% (-----) and 97.5% (------) distribution positions for the log-normal model with parameter dependencies with wave height according to Eq. (11) and the estimated lower limit for T_s (-·-·-) using the measurements.

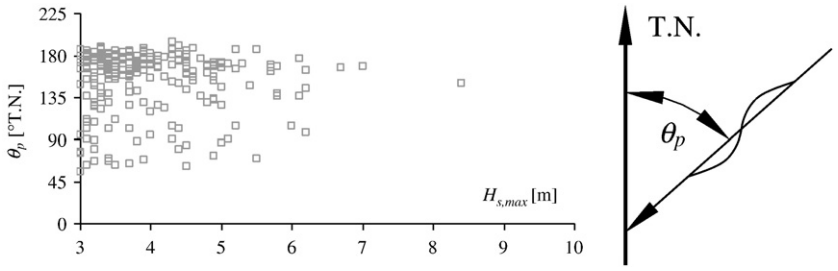

Fig. 8. Left, measured θ_p and $H_{s,max}$ (□) at Long Reef wave buoy, where H_s>3 m. Right, definition sketch for θ_p, which is measured clockwise from true north (N.T.).

0.4 when using the Kaplan–Meier scale ($(i-1/2)/n$, $y_1 \le y_2 \ldots y_i \le y_n$). A more physical model is to fit the Poisson process to the gaps between events. This new non-homogeneous Poisson process is defined using the following notation; if the initial event occurs at $t_{0,s}$ and ends at $t_{0,e}$ and subsequent events starting times at $t_{1,s}$, $t_{2,s}$, …, $t_{n,s}$, with gaps of G_i ($=t_{i,s}-t_{i-1,e} \ge 0$) and using the occurrence intensity $\lambda(t|\boldsymbol{\theta})$, the probability of an event occurring is then

$$F\left(t_{i,s}|t_{i-1,e}\right) = F\left(t_{i-1,e}+G_i|t_{i-1,e}\right) = 1 - e^{-\int_{t_{i-1,e}}^{t_{i-1,e}+G_i}\lambda(t|\boldsymbol{\theta})dt} \quad (15)$$

where $\boldsymbol{\theta}$ is the parameter vector for a particular seasonal occurrence intensity model. Three models for $\lambda(t|\boldsymbol{\theta})$ were tested; $\lambda(t|\boldsymbol{\theta})=\theta_0$ for constant, $\lambda(t|\boldsymbol{\theta})=\theta_0+\theta_1 \sin \omega t+\theta_2 \cos \omega t$ for annual and $\lambda(t|\boldsymbol{\theta})=\theta_0+\theta_1 \sin \omega t+\theta_2 \cos \omega t+\theta_3 \sin 2\omega t+\theta_4 \cos 2\omega t$ for twice-annual occurrence intensity variations where ω is the radian frequency for a 1 year period. The likelihood of Eq. (15) is

$$L(\mathbf{t}|\boldsymbol{\theta}) = \prod_{i=1}^{N}\left[1 - F\left(t_{i-1,e}+G_i|t_{i-1,e}\right)\right]\lambda\left(t_{i-1,e}+G_i|\boldsymbol{\theta}\right) \quad (16)$$

which yields the log-likelihood function of

$$\ell(\mathbf{t}|\boldsymbol{\theta}) = -\sum_{i=1}^{N}\int_{t_{i-1,e}}^{t_{i-1,e}+G_i}\lambda(t)dt + \sum_{i=1}^{n}\ln\left(\lambda\left(t_{i-1,e}+G_i|\boldsymbol{\theta}\right)\right) \quad (17)$$

where $\mathbf{t}$ is the time vector. Maximising Eq. (17) (see Fig. 10) indicates that the annual model is better at the 79% confidence level over the constant model, with the twice-annual model being better at the 5% confidence level over the annual model. Statistical modelling uses the basic rule that unless there is a significantly good reason, the number of model parameters should be minimised (Beirlant et al., 2004; Coles, 2001). The annual occurrence density model has three parameters compared to five in the twice-annual model. These two additional parameters yield a better model compared to the annual model at the 5% confidence level. Another way of saying this is that both the annual and twice-annual models yield equivalent results at the 95% confidence level. Hence, the benefit does not justify the additional complexity introduced by the twice-annual model. Therefore, the annual model was adopted here with $(\hat{\theta}_0, \hat{\theta}_1, \hat{\theta}_2)=(21.46,1.08,1.07)$.

Event clustering, was also investigated, where the next event occurs sooner because the previous event happened. In this scenario, the timing process has a memory, whereas, the Poisson process has no memory. To test event clustering, Luceño et al.'s (2006) approach combined with Eq. (15) for constant, annual and twice-annual seasonal event occurrence intensity was adopted. Their model introduces two additional parameters, γ_0 and γ_1, with $\gamma_0=0$ being equivalent to the non-clustered model. Maximising Eq. (17) with Luceño et al. (2006) yields $\gamma_0=0$ for the three seasonal models. Hence, the measurements do not indicate event clustering. This does not preclude the scenario of two storms occurring close together and consequently producing severe erosion. However, it does imply that there is no evidence within the measurements of temporal dependency other than that already included in the adopted Poisson process. This does not stop erosion events from merging, as the structural function includes the accretion phase which introduces the memory required to encapsulate the antecedent beach condition.

3.1.7. Step 7—simulate the wave climate using the fitted distributions including storm spacing

The extreme wave climate is simulated with the first event at time t, using the Monte Carlo simulation technique and the fitted distributions by repeating the following process; A) generate random realizations of $H_{s,max}$, D, T, θ_p and R; B) estimate beach erosion; C) generate time to next storm; and D) determine profile recovery.

The proposed Monte Carlo simulation requires the generation of random numbers that follow the various target probability density functions. However, available random number generators (e.g., L'Ecuyer, 1994; Park and Miller, 1988) supply a uniform

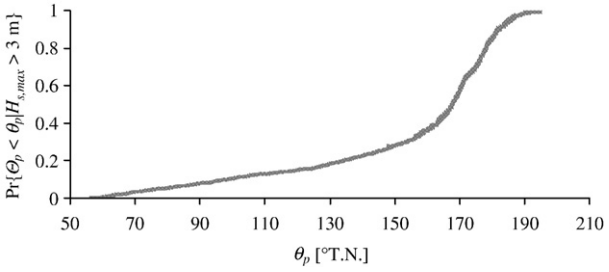

Fig. 9. The empirical cumulative probability for $\theta_p|H_{s,max}$>3 m at Long Reef (see right panel of Fig. 8 for a definition sketch).

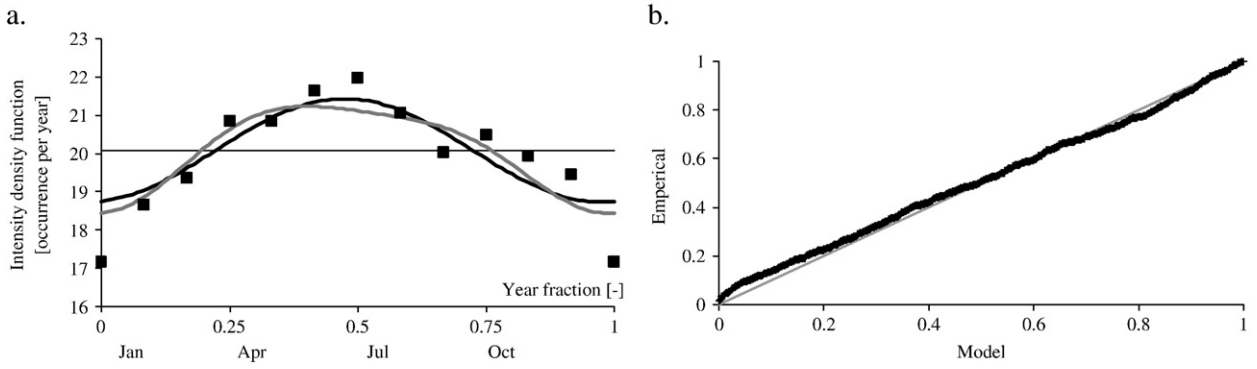

Fig. 10. For the Botany Bay wave buoy; left panel, wave event occurrence for; measured (■) and modelled (Poisson) with constant (—), annual (▬) and twice-annual (▪▪▪▪) variations in event occurrence intensity; and right panel, quantile plot using the Kaplan–Meier scale ($(i-1/2)/N$, $y_1 \le y_2 \ldots y_i \le y_n$) and the modelled annual variation in event occurrence intensity (solid line indicates prefect agreement).

distribution varying from zero to unity and is notated as U(0,1). Given a particular cumulative probability distribution, $F(x)=\Pr\{X<x\}$, we can transform U(0,1) to $F(x)$ by solving

$$F(x) = \Pr\{X < x\} = A \tag{18}$$

for x (see Fig. 11a) where $A \sim \mathrm{U}(0,1)$. Analytical solutions of Eq. (18) are possible when the indefinite integral of $\frac{\partial F(x)}{\partial x}$ is known and invertible. The following section provides the additional formulations required in the Monte Carlo simulation to handle the situations when complications arise with either integrating $\frac{\partial F(x)}{\partial x}$ or solving Eq. (18).

The generation of dependant Fréchet pairs for ($H_{s,max}$,D) and ($H_{s,max}$,R) uses the Gibbs sampling technique (Geman and Geman, 1984) as follows, using x for $H_{s,max}$, y for D and z for R;

1. generate y_0 using $A \sim (0,1)$ and $y_0 = -(\ln A)^{-1}$;
2. for the ith storm;
   a. generate $(A, B, C) \sim \mathrm{U}(0,1)$;
   b. transform A to the Fréchet scale with dependency α ($H_{s,max}$ and D), by solving

$$\begin{aligned} A &= \Pr\{X \le x_i | Y = y_{i-1}\} \\ &= \left(x_i^{-\alpha^{-1}} + y_{i-1}^{-\alpha^{-1}}\right)^{\alpha-1} y_{i-1}^{\alpha-1/\alpha} e^{-\left(x_i^{-\alpha^{-1}} + y_{i-1}^{-\alpha^{-1}}\right)^{\alpha} + y_{i-1}^{-1}} \end{aligned} \tag{19}$$

   for x_i using numerical methods (e.g., Brent, 1973);
   c. transform B to the Fréchet scale with dependency α ($H_{s,max}$ and D), by solving

$$\begin{aligned} B &= \Pr\{Y \le y_i | X = x_i\} \\ &= \left(x_i^{-\alpha^{-1}} + y_i^{-\alpha^{-1}}\right)^{\alpha-1} x_i^{\alpha-1/\alpha} e^{-\left(x_i^{-\alpha^{-1}} + y_i^{-\alpha^{-1}}\right)^{\alpha} + x_i^{-1}} \end{aligned} \tag{20}$$

   for y_i;
   d. transform C to the Fréchet scale with dependency α ($H_{s,max}$ and R), by solving

$$\begin{aligned} C &= \Pr\{Z \le z_i | X = x_i\} \\ &= \left(x_i^{-\alpha^{-1}} + z_i^{-\alpha^{-1}}\right)^{\alpha-1} x_i^{\alpha-1/\alpha} e^{-\left(x_i^{-\alpha^{-1}} + z_i^{-\alpha^{-1}}\right)^{\alpha} + x_i^{-1}} \end{aligned} \tag{21}$$

   for z_i;
   e. transform Fréchet x_i, y_i and z_i to the physical scale (i.e., $H_{s,max}$, D and R) using the marginal distributions, e.g.,

$$\mathrm{Tr}\{w\} = \begin{cases} u + \dfrac{\sigma}{\xi}\left[\left\{\dfrac{1-e^{-\frac{1}{w}}}{\zeta_u}\right\}^{-\xi} - 1\right] & \xi \neq 0 \\ u - \sigma \ln\left\{\dfrac{1-e^{-\frac{1}{w}}}{\zeta_u}\right\} & \xi = 0 \end{cases} \quad e^{-\frac{1}{w}} \ge 1-\zeta_u$$
$$\text{empirical distribution} \qquad e^{-\frac{1}{w}} < 1-\zeta_u \tag{22}$$

   where w is the Fréchet deviate. As indicated by Eq. (22), the empirical distribution is used to define the probability distribution function, $\Pr\{X \le x\}$ when $X \le u$ (see Fig. 11b).

The Gibbs sampling technique requires a number of iterations before the random realisations convergence to a Markov Chain. From testing, 1000-cycles yields acceptable convergence. To ensure this convergence is not an issue in the simulations, we waste the first 10,000-cycles.

T_s is generated from the log-normal distribution using Eq. (11) to define the distribution parameters (κ, μ, σ). The Box–Müller method (Box and Muller, 1958) is used to generate two random deviates with standard normal distribution (zero mean and standard deviation of unity) from two uniformly distributed variates. This method is adapted to yield two log-normal distributed variates using;

1. generate two uniform random variables $(A', B') \sim \mathrm{U}(0,1)$ and transform them into the unit circle around the origin $(A, B) = (2A'-1, 2B'-1)$; and check that the radius, R given by $R^2 = A^2 + B^2$ satisfies $R \in [0; 1]$ otherwise generate new (A', B') and repeat this step;
2. calculate the standard normal random variables $(C, D) = (f_{sn} A, f_{sn} B)$ where $f_{sn} = \sqrt{\frac{-2\ln R^2}{R^2}}$; and
3. transfer one of the normal random variate to the wave period using $\mathrm{Tr}\{w\} = \kappa e^{\mu - \sigma w}$ and save the other normal random variate for future use.

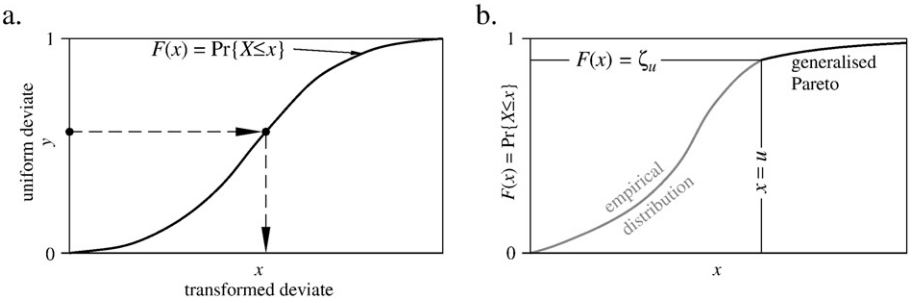

Fig. 11. a) Transformation of a uniform random deviate $y \sim U(0,1)$ to a known probability distribution $\frac{\partial F(x)}{\partial x}$ (after Press et al., 1992) and b) the empirical and generalised Pareto distributions used in the Monte Carlo simulation.

G, the time to the next event (storm spacing), is generated as follows;

1. generate a uniform deviate $A \sim U(0, 1)$;
2. solve Eq. (15) for G_i with $F(...)=A$ using annual variations in event occurrence intensity. Completing the integrations of Eq. (15) and simplifying yields

$$F(G_i) = 1 - e^{\frac{\theta_0 \omega G_i + \theta_1 \left(\cos \omega t_{i-1,e} - \cos \omega \left(t_{i-1,e}+G_i\right)\right) - \theta_2 \left(\sin \omega t_{i-1,e} - \sin \omega \left(t_{i-1,e}+G_i\right)\right)}{\omega}} \tag{23}$$

An initial estimate can be obtained from the second order Taylor series expansion about $G_i=0$ of Eq. (23), i.e.,

$$G_{i,\text{initial}} = \frac{A}{\theta_0 + \theta_1 \sin\ \omega t_{i-1,e} + \theta_2 \cos \omega t_{i-1,e}}. \tag{24}$$

The high speed bounded root solver developed by Brent (1973) was used in combination with the initial guess and knowing that $G_i>0$ to estimate the root boundaries. Other methods like Newton–Raphson were found to sporadically find negative roots, which are non-physical.

The simulation length generated depends on the accuracy desired at a given return level. For example, to estimate 100-year return levels using simulation only, then simulation of at least 400 years is required with most authors recommending between 400 and 1000-years (see Hawkes, 2000 and references therein). However, the length required to estimate extreme values accurately should be investigated through convergence testing as much longer simulations are required when searching several extreme tails.

Fig. 12 shows the dependency between various variates and $H_{s,max}$ for an 1000-year simulation. These scatter plots indicate some minor discrepancy when visually compared with measurements (comparing panels a, b, c and d with Figs. 4, 8, 6 and 5 respectively). Comparing the fitted and simulated marginal distributions indicates that the logistic dependency model is not distorting the marginal distributions of $H_{s,max}$, D

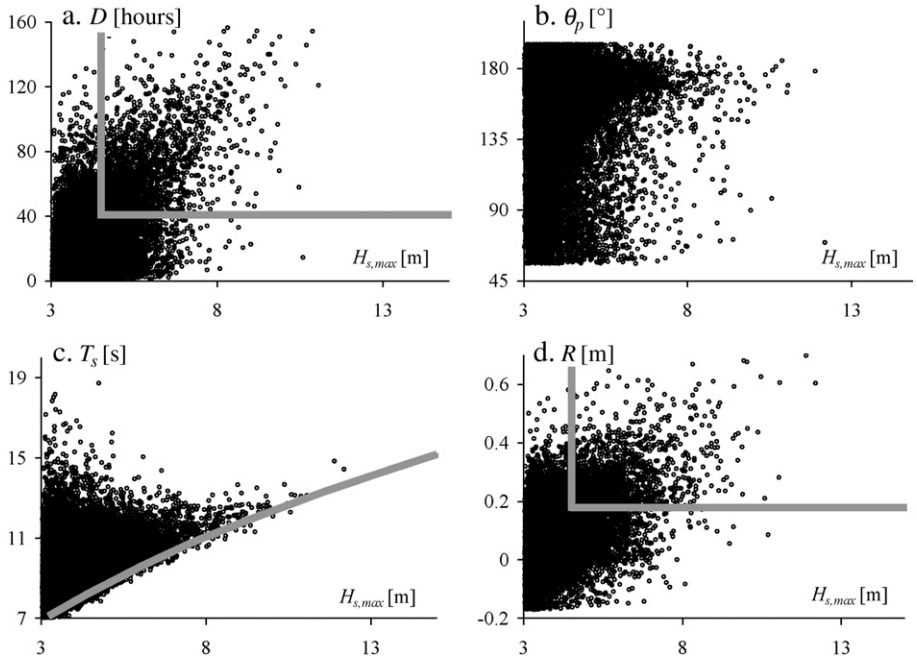

Fig. 12. 1000-years example simulation for a. D (GP using Botany Bay), b. θ_p (empirical using Long Reef), c. T_s (variable log-normal using Botany Bay) and d. R (GP using Fort Denison). The continuous lines in panels a and d are thresholds used in the GP distributions, with empirical distributions used below these thresholds (see Fig. 11b).

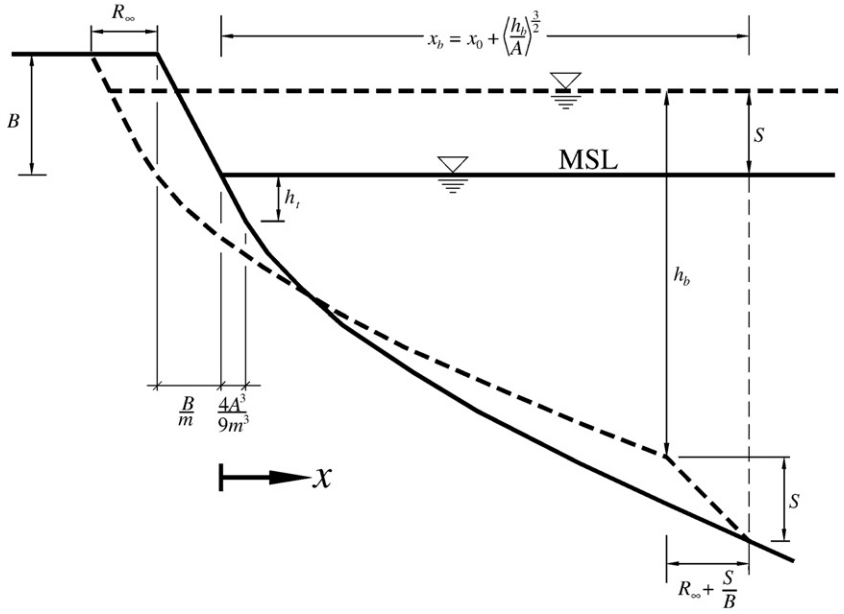

Fig. 13. The maximum beach regression (R_∞) from a water-level surge (S) using the composite profile shape given by Eq. (25) (after Kriebel and Dean, 1993).

and R (not shown). At this stage, we have not pursued further statistical refinement for the following practical reasons; we have already simplified the manner in which D is applied in the erosion model; the variably in the storm shapes has been ignored; and estimating beach erosion and accretion involves errors that are generally factor two or more, where as, the errors within the simulation are typically small. We consider the simulated climate a reasonable approximation to the measured climate for the purposes of beach erosion. However, other approaches for modelling dependency between variates that can improve the statistical modelling are the two parameter bilogistics (Coles, 2001) or the seven parameter mixture of bivariate normals models (Hawkes, 2000; Hawkes et al., 2002).

3.2. Structural function (Step 8—estimate extreme values of beach erosion from the simulated wave climate)

The full temporal simulation method requires a structural function to convert the synthetic climate record into the quantity being investigated. In this study, the quantity under investigation is beach erosion from incident storms with wave periods between 5 and 20 s. The structural function used to estimate this quantity is based on the equilibrium profile concept. The equilibrium profile used by Kriebel and Dean (1993) is (see Fig. 13)

$$h = \begin{cases} -B & x \le -\dfrac{B}{m} \\ mx & -\dfrac{B}{m} \le x \le \dfrac{4A^3}{9m^3} \\ A(x-x_0)^{\frac{2}{3}} & x \ge \dfrac{4A^3}{9m^3} \end{cases} \tag{25}$$

where h is the water depth, x is the cross-shore coordinate, increasing offshore, B is the dune height above mean sea level (MSL) and A is an empirical coefficient (see Dean and Dalrymple, 2002 for a recent summary). This profile shape has a virtual origin at $x_0 = 4/27A^3m^{-3}$ with the region where wave energy dissipation per unit volume is constant ($h \propto x^{2/3}$) occurring offshore of $x_s = 4/9A^3m^{-3}$. The maximum eroded volume after exposure to an increase in mean water level is

$$V_\infty = \begin{cases} R_\infty B & z > S - 4/9A^3m^{-2} \\ \left.\begin{array}{l} R_\infty B + \dfrac{h_t^2 - 2Sh_t + S^2 - z^2}{2m} \\ + \dfrac{8A^3(15Sm^2 - 4A^3)}{405m^5} - \dfrac{\sqrt{S-z}(2S^2 + Sz - 3z^2)}{5A^{3/2}} \end{array}\right\} & z \le S - 4/9A^3m^{-2} \end{cases} \tag{26}$$

where S is the vertical shift in the equilibrium profile if the mean water level were to change permanently (see Fig. 13), $h_t = \frac{4A^3}{9m^2}$, the depth at the transition from constant to $\frac{2}{3}(x-x_0)^{-\frac{1}{3}}$ beach slope, z is the elevation of the seaward boundary contour (see Fig. 14a) and

$$R_\infty = \frac{S\left(x_0 + \left[\frac{h_b}{A}\right]^{\frac{3}{2}} - \frac{h_b}{m}\right)}{B + h_b - \frac{1}{2}S} \tag{27}$$

with h_b being the water depth at wave breaking. Fig. 14a and b shows the beach volume before and after a storm with panel c illustrating the eroded volume, V_∞, given by Eq. (26), which is the subaerial volume change above MSL ($z_b = 0$ in Fig. 14) and landward of the $z = 2$ m contour. This volume change is consistent with that historically used by researchers investigating beach erosion along the New South Wales coast (see for example, page 95 of Hoffman and Hibbert, 1987).

Kriebel and Dean (1993) showed that short duration wave events do not achieve V_∞. Using a linear response for beach

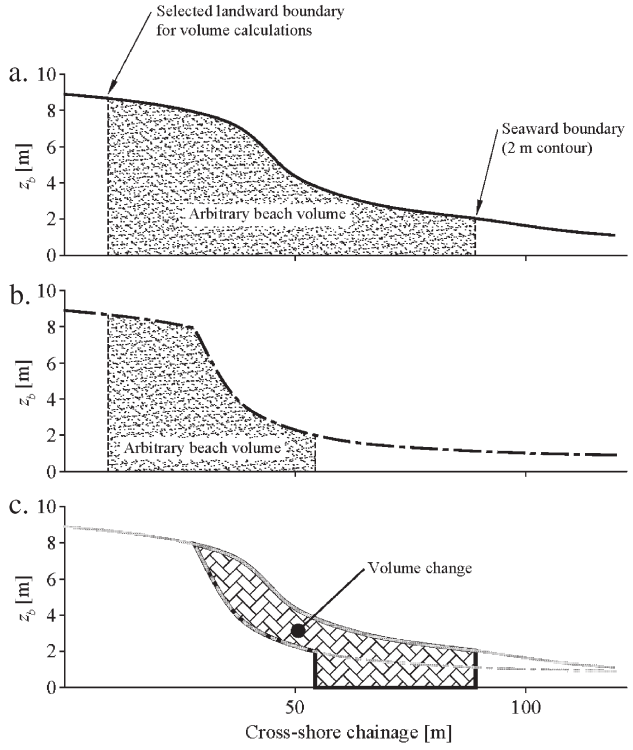

Fig. 14. Beach volume change definition sketch after Hoffman and Hibbert (1987) for a. Pre-storm, b. Post-storm and c. Beach volume change.

recessions, Kriebel and Dean (1993) solved for the temporal behaviour using the convolution integral approach as follows,

$$V(t)=\begin{cases} V_{\text{intial}}e^{-\frac{t}{T_{s,a}}} & 0\le t\le t_s \\ \dfrac{V_\infty}{T_{s,e}}\displaystyle\int_0^t f(\tau)e^{-\frac{t-\tau}{T_{s,e}}}d\tau & t_s<t\le t_m \\ V(t=t_m)e^{-\frac{t-t_m}{T_{s,a}}} & t>t_m \end{cases} \quad (28)$$

with $f(t)=\sin^2 \pi t/D$ where t is time measured from the start of a particular storm; V_{initial} is the initial eroded sand volume; $T_{s,e}$ and $T_{s,a}$ are the characteristic time scales of the exponential response under erosive (see Kriebel and Dean, 1993) and accretive (taken as $T_{s,a}=400$ h, conservatively estimated using the measurements from Ranasinghe et al. (2004)) conditions respectively; t_s is the time when storm erosion is greater than the initial erosion; t_m is the time of maximum erosion during the storm and $f(t)$ is the storm shape function. The storm duration (D in storm shape function, $f(t)$) qualitatively affects the beach erosion amount as follows; larger D, the more time the beach has to achieve the new equilibrium form and consequently more chance that V_∞ that will be achieved. The wave period (T_s) and direction (θ_p) enter Eq. (28) via wave propagation from deep water to the breaking point (refraction and shoaling processes), which affects the depth at which waves break (h_b) and consequently R_∞ and $T_{s,e}$ (the erosion response time). Fig. 15 shows an application of Eq. (28) in which two independent meteorological events (waves) are merged into one erosional event.

The approach used to apply Eq. (28) is;

1. initially assume $V_{\text{initial}}=0$ for $i=1$;
2. estimate the maximum change in mean water level using the simulated wave climate for event i, being the addition of;
   a. tidal anomaly; and
   b. additional wave set-up over non-storm conditions;
3. estimate H_b, h_b and x_b (wave height, water depth and position of the wave breaking point) using
   a. spectral wave propagation model to transfer the wave measurements from offshore to the nearshore (we use the 20 m depth contour as our nearshore position); and
   b. use linear wave theory and assume parallel contours from the nearshore wave conditions to the wave breaking point;
4. calculate $T_{s,e}=320\frac{H_b^{3/2}}{\sqrt{g}A_{eq}^3}\left(1+\frac{h_b}{B}+\frac{mx_b}{h_b}\right)^{-1}$ (Kriebel and Dean, 1993);
5. solve for t_m using Eq. (28);
6. calculate V_{initial} for the next storm event; and
7. repeat steps 2–6.

This method requires estimation of two additional parameters, the wave breaking depth h_b and set-up due to the breaking waves (the total surge S, being the sum of the storm surge and the additional wave set-up). The breaking water depth was determined when the local wave height exceed $\gamma_b h$. The wave set-up was estimated assuming a static, shore-normal force balance between wave radiation stress and pressure gradients generated by the sloping mean water surface. The wave set-up ignores wind and bed shear stresses and assumes saturated wave breaking conditions ($H(x)=\gamma_b h(x)$ shoreward of the breaking point). The resulting maximum set-up, $\overline{\eta}_{\max}$, under these conditions is

$$\overline{\eta}_{\max}=\frac{40-3\gamma_b^2}{128}\gamma_b H_b \quad (29)$$

and using $\gamma_b=0.78$ yields $\overline{\eta}_{\max}\approx 0.23H_b$, where H_b is the wave height where breaking initially occurs (Dean and Dalrymple, 1991).

The Kriebel and Dean (1993) model requires the change in key parameters that occur when moving from average to storm conditions. That is, the equilibrium profile has already taken into account the astronomical tide and the average wave conditions. Consequently, the model is driven by the change in the mean

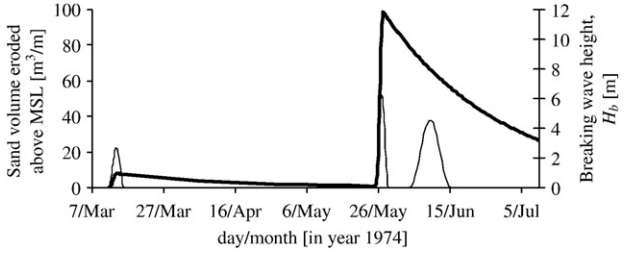

Fig. 15. Example application of Eq. (28) showing the breaking wave height (—) and exponential beach erosion response (▬) using $T_s \in [8; 12]$ hours during the May/June 1974 storms (Foster et al., 1975) at Narrabeen Beach, Sydney.

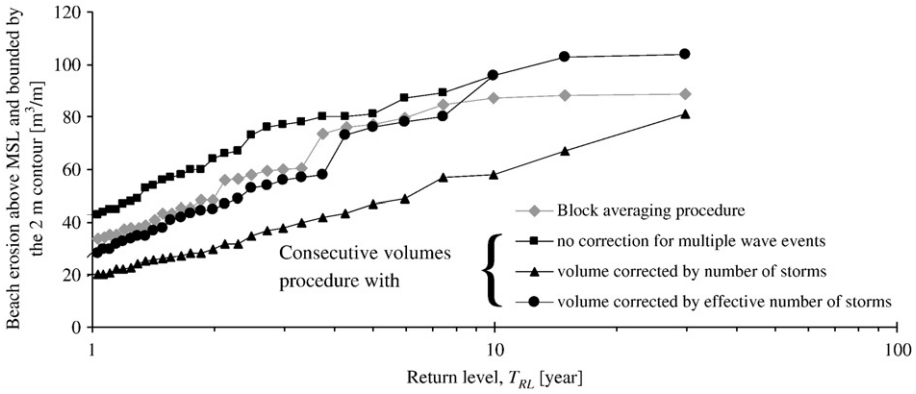

Fig. 16. Beach erosion above MSL empirical estimates for Narrabeen Beach profile 4 (Short and Trembanis, 2004) for the block averaging (gray) and consecutive volumes (black) procedure.

water level (see step two in the above procedure). The beach erosion method adopted by FEMA for the south-western coast of the USA uses this approach (see equation D.4.6-2 of FEMA, 2004). This method may over or under predict beach erosion for short duration storms (durations much less than one tidal period) that occur at low or high tide respectively. However, the typical storm duration that produces noteworthy erosion at Narrabeen Beach persist for several days and hence, the impact of this simplification is expected to be averaged out. Nevertheless, more complicated erosion models are available and can be used as a substitute for the Kriebel and Dean (1993) model.

4. Field measurements

The rare profile measurements at Narrabeen Beach (Short and Trembanis, 2004) conducted from 27 April 1976 until 2 March 2006 were used to assess this approach by comparing measured with predicted extreme erosion volumes. Profile 4, located near the beach rotation fulcrum (Short and Trembanis, 2004) was selected as longshore erosion effects are minimal and the (beach) sand supply is plentiful. Two methods were used to estimate extreme storm erosion volume statistics at profile number 4 (see Fig. 1c). The first approach, referred to as block averaging, uses the following procedure;

1. for each 1.5 month period, starting at the first measurement, determine the average volume above MSL and bounded by the 2 m contour and profile origin (as per Fig. 14);
2. when required, interpolate missing values;
3. calculate volume change between each 1.5 month block; and
4. determine maximum value from step 3 in each 12 month period.

The Narrabeen Beach profile sampling interval varies from between 2 days through to 124 days with 85% being less than 1.5 months apart. Consequently, a block period of 1.5 months was chosen to ensure that most blocks will have at least one measurement in them. This block averaging procedure was undertaken as consecutive profile measurements typically encompass several wave events (average wave event spacing is 2.6 weeks compared to profile survey spacing of *ca* 5 weeks). Using this procedure is expected to introduce a bias. This bias may be minor if typically only one of the storms between profile measurements is very extreme.

The second approach, referred to as consecutive volumes, uses Botany Bay wave measurements to identify the time that storms occurred. The erosion volume relevant to each individual storm was then obtained from the consecutive profiles bracketing the wave event or events. This method resulted in;

- the identification of 268 erosion events (i.e., one or more storms occurred between consecutive profile measurements);
- 19 profile measurements were not included (these are the profiles associated with calm periods);
- the average time gap between the pre-profile and the first wave event starting was 11 days;
- the average time gap between the last wave event finishing and the post-profile was 10 days; and
- the average time gap between consecutive profile measurements was 35 days.

In order to handle multiple wave events between consecutive profiles, three correction methods were investigated. They are; (a) no correction; (b) dividing the erosion volume by the number of identified wave events between consecutive profile measurements; and (c) dividing the erosion volume by the effective number of wave events between consecutive profile measurements. The effective number of wave events was subjectively estimated using the following rules-of-thumb; if there was one or more big events compared to the others, count only the big events; otherwise remove small events compared to the remaining events; and if unclear, count all events.

The return period of the volume changes are given by

$$T_{\mathrm{RL}} = \frac{1}{\frac{i}{N+1}\times\frac{N}{Y}} \approx \frac{Y}{i} \text{ for } N>100 \tag{30}$$

for the ith largest event ($x_1 \geq \ldots \geq x_i \geq \ldots \geq x_N$), where T_{RL} is return period in years, N is the number of events and Y is the measurement period in years. Fig. 16 shows the erosion volumes against return period using both procedures. The block averaging procedure lies between the consecutive volumes procedure with

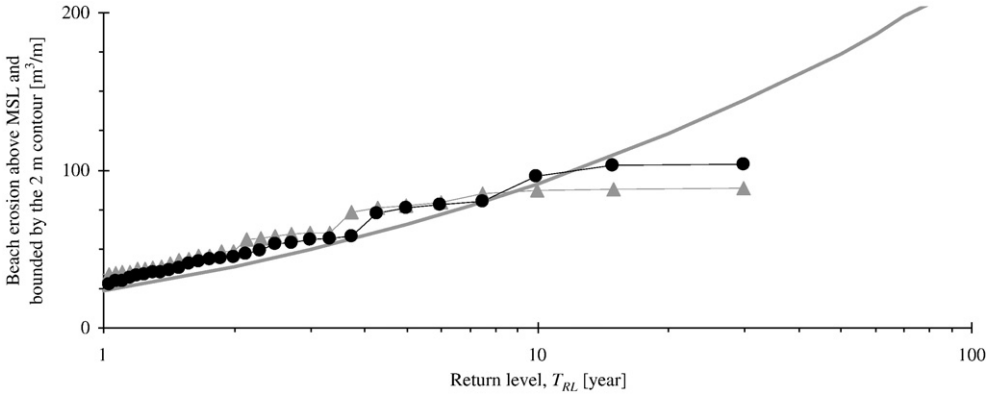

Fig. 17. The eroded sand volume above MSL at Narrabeen Beach from; profile measurements (—◆— and —●— defined on Fig. 16); and using steps 1–8 (—) and simulating 50,000 years to ensure convergent predictions.

no correction and correction based on the total number of storms between measurements. However, correcting the consecutive volumes procedure where it contains several wave events by using the effective number of storms yielded predictions similar to the block averaging procedure.

It is concluded that both procedures have bias due to the large temporal interval between profile measurements that resulted in consecutive measurements bracketing more than one wave event. For the 30 largest consecutive volume changes at profile 4, 20% have a single wave event compared to 26.7%, 13.3% and 30% having two, three or four wave events respectively between profile measurements. The remaining 10% have five or more wave events between consecutive measurements. Given the lack of long term measurements on beach profile changes suitable for estimating extreme statistics, we accept the shortcoming of this measurement set on the basis that quantitative consistency between the two procedures (—◆— and —●— on Fig. 16) suggests some reliance is justified.

As previously mentioned, the Narrabeen Beach measurements cover approximately 30 years. Hence, the estimation of extreme erosion statistics (Fig. 16) is well predicted up to *ca* 7.5 years with subsequent predictions heavily effected by sampling error (i.e., the population is not well represented for return periods exceeding 7.5 years).

5. Results

The proposed method presented in Section 3 was applied to estimate erosion volumes at Narrabeen Beach at profile 4, which is located mid-way between the headlands forming this embayment beach (see Fig. 1). The wave parameters and water levels used to demonstrate the various statistical models were adopted for this location. The Kriebel and Dean (1993) profile model parameters are $A=0.14$ m$^{1/3}$, obtained from the measured medium sand grain diameter and using Dean and Dalrymple (2002), the beachface slope, $m=0.07$ and dune height above mean sea level, $B=10$ m was obtained from profile surveys. The nearshore wave heights and directions were translated from the wave buoy location using a spectral wave model with measured bathymetry. The method provided in Section 3.2, including the wave breaking criteria and the wave set-up estimation formulation, was used to apply the structural function. Fig. 17 shows that the predictions from the proposed method were able to reproduce the quantitative behaviour of the measured extreme erosion values at Narrabeen Beach. This is remarkable in that the structural function used in this article is an exceptionally simple erosion/accretion model. At this stage, the confidence limits on the erosion volumes have not been estimated. It is expected, however, that the confidence limits are wide for large return periods. For example, the wave height 95% confidence limits (see Fig. 3a) for the 100 year return period are a factor 0.87 and 1.4 of the predicted quantity. Similarly large confidence ranges exist for event duration and tidal anomaly. How these uncertainties combine is a complex matter and determining them is outside the scope of this paper. Nevertheless, it is expected that the confidence limits will exceed the ratio width determined for the peak wave height ($H_{s,max}$).

6. Conclusions

Coastline management often requires the accurate quantification of storm erosion and inundation hazards. The benchmark approach in which a representative (worst case) event is used has been replaced by a method that includes event merging and can incorporate climate change impacts. For example, increased storm intensity can be modelled by modifying $\lambda(t|\boldsymbol{\theta})$ in Eq. (15). The main advantages of this probability based method compared to the benchmark storm approach are; (a) incorporation of storm duration and (b) the probabilities for a range of erosion volumes are determined and not inferred from one of the forcing variates.

The full temporal simulation method used here includes the following three main steps; the simulation of forcing variates from statistical models that include the joint probability between key variates; the simulation of the time between storms using a non-homogenous Poisson process; and the simulation of each event to determine the erosion amount. This method was demonstrated using climate information (waves and tides) obtained at Botany Bay and Long Reef (both near Sydney) and the simple erosion/accretion model after Kriebel and Dean (1993).

Comparison with the extreme beach erosion volumes at Narrabeen Beach, Sydney, confirmed that the statistical approach is capable of reproducing the measurements for return periods up to 10 years. Improvements in the method accuracy would be achievable by longer measurement records of the forcing variates (statistical component); and improving the erosion model formulation (structural function component).

Nevertheless, the presented measurements, wave transformation and erosion modelling have produced erosion estimates from the full simulation method that suggests this framework is suitable for determining coastal erosion hazard due to storms. It should be noted that this method does not include chronic and ongoing erosion sources (see for example Zhang et al., 2004).

7. Future directions

The application of Kriebel and Dean (1993) to determine beach erosion is one aspect of this work that presents a clear limitation. At higher return periods, the predicted erosion value increases at an ever increasing rate (upwards concave). This feature is not considered realistic. Consequently, more detailed profile modelling is being undertaken to investigate whether this aspect of the structural function is critical for providing accurate predictions using the proposed framework.

Improvements to the statistical approach would also provide improvements in the simulated climate. The areas for improvement in the climate modelling are; the dependency modelling between wave height, storm duration and tidal anomaly; separating out the statistical modelling based on meteorological conditions generating the waves and re-combing them during the simulation phase; supplementing wave measurements with hindcasted parameters to improve statistical fits; and incorporating realistic temporal variation of wave parameters. However, the improvement from this group of changes is expected to be minor when compared to that obtained by refining the profile change model.

The method presented can be extended to estimate confidence limits by bootstrapping (Markus, 1994) steps 1–8. The basic principal of bootstrapping is that the sample is assumed to represent the population and new samples are randomly formed from that population. The challenge will be to apply this framework in a timely manner, as bootstrapping typically required 10^3 to 10^4 cycles.

Acknowledgements

The Sydney tidal anomalies (Fort Denison) and waves (Long Reef) were provided by Manly Hydraulic Laboratory on behalf of the NSW Department of Environment and Climate Change (Messrs M. Kulmer and P. Murphy). The Botany Bay offshore wave measurements were provided by Sydney Port (Mr G. Batman). This work is financially funded by NSW Department of Environment and Climate Change through the Natural Disaster Mitigation Programme.

We gratefully acknowledge the useful, critical and constructive comments and suggestions on the manuscript by the anonymous reviewers and Dr Tom Baldock.

References

Alves, G.M.J.H., Young, I.R., 2003. On estimating extreme wave heights using combined Geosat, Topex/Poseidon and ERS-1 altimeter data. Applied Ocean Research 25 (4), 167–186.

Anonymous, 1995. New South Wales ocean tide levels annual summary 1994/95. Department of Public Works and Services Report number 95121, Manly Hydraulics Laboratory Report number MHL732, Manly Vale, NSW.

Behrens, C.N., Lopes, H.F., Gamerman, D., 2004. Bayesian analysis of extreme events with threshold estimation. Statistical Modelling: An International Journal 4 (3), 227–244.

Beirlant, J., Goegebeir, Y., Teigels, J., Segers, J., De Wall, D., Ferro, C., 2004. Statistics of Extremes. John Wiley & Sons Ltd, West Sussex. Wiley Series in Probability and Statistics, 490 pp.

Box, G.E.P., Muller, M.E., 1958. A note on the generation of random normal deviates. The Annals of Mathematical Statistics 29 (2), 610–611.

Brent, R.P., 1973. Algorithms for Minimization without Derivatives. Prentice-Hall, Englewood Cliffs, N.J. Prentice-Hall Series in Automatic Computation, 195 pp.

Bruun, J.T., Tawn, J.A., 1998. Comparison of approaches for estimating the probability of coastal flooding. Applied Statistics 47 (3), 405–423.

Coles, S., 2001. An Introduction to Statistical Modelling of Extreme Values. Springer, London. Springer Series in Statistics, 216 pp.

Coles, S., 2004. Chapter 2, the use and misuse of extreme value models in practice. In: Finkenstädt, B., Rootzén, H. (Eds.), Extreme Values in Finance, Telecommunications, and the Environment. Chapman & Hall/CRC, Boca Raton, pp. 79–100.

Coles, S.G., Tawn, J.A., 1991. Modelling extreme multivariate events. Journal of the Royal Statistical Society. Series B, Statistical Methodology 53 (2), 377–392.

Coles, S., Pericchi, L., 2003. Anticipating catastrophes through extreme value modelling. Journal of the Royal Statistical Society. Series C, Applied Statistics 52 (4), 405–416.

Coles, S., Tawn, J., 2005. Bayesian modelling of extreme surges on the UK east coast. Philosophical Transactions – Royal Society. Mathematical, Physical and Engineering Sciences 363 (1831), 1387–1406.

Davidson, R., MacKinnon, J.G., 2004. Econometric Theory and Methods. Oxford University Press, New York. xviii, 750 p.

Davison, A.C., Smith, R.L., 1990. Models for exceedances over high thresholds. Journal of the Royal Statistical Society. Series B, Statistical Methodology 52 (3), 393–442.

Dawson, T.H., 2000. Maximum wave crests in heavy seas. Journal of Offshore Mechanics and Arctic Engineering – Transactions of the AMSE 122 (3), 222–224.

Dean, R.G., Dalrymple, R.A., 1991. Water Wave Mechanics for Engineers and Scientists. Advanced Series on Ocean Engineering, vol. 2. World Scientific, Singapore. 353 pp.

Dean, R.G., Dalrymple, R.A., 2002. Coastal Processes with Engineering Applications. Cambridge University Press, Cambridge. xi, 475 pp.

FEMA, 2004. Final Draft Guidelines for Coastal Flood Hazard Analysis and Mapping for the Pacific Coast of the United States. FEMA and northwest hydraulic consultants.

Foster, D.N., Gordon, A.D., Lawson, N.V., 1975. The Storms of May–June 1974, Sydney, N.S.W., Proceedings of the 2nd Australasian Coastal and Ocean Engineering Conference. The Institution of Engineers, Australia, Gold Coast, Australia, pp. 1–11.

Garrity, N.J., Battalio, R., Hawkes, P.J., Roupe, D., 2006. Evaluation of event and response approaches to estimate the 100-year coastal flood for pacific coast sheltered waters. In: J. McKee Smith, Proceedings of the 30th International Conference on Coastal Engineering. World Scientific, San Diego, USA, pp. 1651–1662.

Geman, S., Geman, D., 1984. Stochastic relaxation, Gibbs distributions and the Bayesian restoration of images. IEEE Transactions on Pattern Analysis and Machine Intelligence PAMI-6 (6), 721–741.

Goda, Y., 1988. On the methodology of selecting design wave height. In: B.L. Edge, Proceedings of the 21st International Conference on Coastal Engineering. ASCE, pp. 899–913.

Hawkes, P.J., 2000. The joint probability of waves and water levels: JOIN-SEA: a rigorous but practical new approach. Report SR 537, HR Wallingford, Oxford.

Hawkes, P.J., Gouldby, B.P., Tawn, J.A., Owen, M.W., 2002. The joint probability of waves and water levels in coastal engineering design. Journal of Hydraulic Research 40 (3), 241–251.

Hoffman, J., Hibbert, K., 1987. Collaroy/Narrabeen beaches, coastal process hazard definition study, 1. Public Works Department, Coastal Branch, N.S.W., PWD Report No. 87040, Sydney, 157 pp.

ICSM, 2002. Geocentric datum of Australia. Technical manual, version 2.2, Inter-governmental Committee on Surveying and Mapping, Canberra.

Kamphuis, J.W., 2000. Introduction to Coastal Engineering and Management, vol. 16. World Scientific, Singapore. Advanced series on ocean engineering, 437 pp.

Kriebel, D.L., Dean, R.G., 1993. Convolution method for time-dependent beach-profile response. Journal of Waterway, Port, Coastal and Ocean Engineering 119 (2), 204–226.

Kulmar, M., Lord, D., Sanderson, B., 2005. Future directions for wave data collection in New South Wales. In: M. Townsend, D. Walker, Proceedings of the 17th Australasian Coastal and Ocean Engineering Conference and the 10th Australasian Port and Harbour Conference. The Institution of Engineers, Australia, Adelaide, South Australia, pp. 167–172.

L'Ecuyer, P., 1994. Uniform random number generation. Annals of Operation Research 53 (1), 77–120.

Lasdon, L.S., Waren, A.D., Jain, A., Ratner, M., 1978. Design and testing of a generalized reduced gradient code for nonlinear programming. ACM Transactions on Mathematical Software 4 (1), 34–50.

Lawson, N.V., Abernethy, C.L., 1975. Long term wave statistics off Botany Bay, Proceedings of the 2nd Australasian Coastal and Ocean Engineering Conference. The Institution of Engineers, Australia, Gold Coast, Australia, pp. 167–176.

Lord, D., Kulmar, M., 2000. The 1974 storms revisited: 25 years experience in ocean wave measurements along the south-east Australian coast. In: B.L. Edge, Proceedings of the 27th International Conference on Coastal Engineering. ASCE, Sydney, Australia, pp. 559–572.

Luceño, A., Menéndez, M., Méndez, F., 2006. The effect of temporal dependence on the estimation of the frequency of extreme ocean climate events. Proceedings of the Royal Society of London, Series A 462 (2070), 1683–1697.

Markus, M.T., 1994. Bootstrap Confidence Regions in Nonlinear Multivariate Analysis. DSWO Press, Leiden University, Leiden, The Netherlands. 201 pp.

Mathiesen, M., Goda, Y., Hawkes, P.J., Mansard, E., Martin, M.J., Peltier, E., Thompson, E.F., Vledder, G.V., 1994. Recommended practice for extreme wave analysis. Journal of Hydraulic Research 32 (6), 803–814.

Méndez, F., Menéndez, M., Luceño, A., Losada, I.J., 2006. Estimation of the long-term variability of extreme significant wave height using a time-dependent Peak Over Threshold (POT) model. Journal of Geophysical Research 111 (C07024), 1–13.

Morton, I.D., Bowers, J., Mould, G., 1997. Estimating return period wave heights and wind speeds using a seasonal point process model. Coastal Engineering 31 (1–4), 305–326.

Nelder, J.A., Mead, R., 1965. A simple method for function minimization. Computer Journal 7, 308–313.

Park, S.K., Miller, K.W., 1988. Random number generators: good ones are hard to find. Communications of the ACM 31 (10), 1192–1201.

Press, W.H., Teukolsku, S.A., Vetterling, W.T., Flannery, B.P., 1992. Numerical recipes in FORTRAN: the art of scientific computing. Cambridge University Press, Cambridge. 1486 pp.

Ranasinghe, R., Symonds, G., Black, K., Holman, R., 2004. Morphodynamics of intermediate beaches: a video imaging and numerical modelling study. Coastal Engineering 51 (7), 629–655.

Shi, D., 1995. Fisher information for a multivariate extreme value distribution. Biometrika 82 (3), 644–649.

Short, A.D., Trembanis, A.C., 2004. Decadal scale patterns in beach oscillation and rotation Narrabeen Beach, Australia—time series, PCA and wavelet analysis. Journal of Coastal Research 20 (2), 523–532.

Short, A.D., Trenaman, N.L., 1992. Wave climate of the Sydney region, an energetic and highly variable ocean wave regime. Australian Journal of Marine and Freshwater Research 43 (4), 765–791.

Tawn, J.A., 1988. Bivariate extreme value theory: model and estimation. Biometrika 75 (4), 397–415.

Trindade, J., Holthuijsen, L., Atkins, G.N., Banks, L.R., 1993. Modelling wave penetration in Botany Bay, Proceedings of the 11th Australasian Conference on Coastal and Ocean Engineering. National Conference Publication – Institution of Engineers, Australia. The Institution of Engineers, Australia, Townsville, Australia, pp. 65–70.

Youll, P.H., 1981. Botany Bay waverider system-10 years of records. In: R. Silvester et al., Proceedings of the Fifth Australian Conference on Coastal and Ocean Engineering. The Institution of Engineers, Australia, Perth, Australia, pp. 245–251.

Zhang, K., Douglas, B.C., Leatherman, S.P., 2004. Global warming and coastal erosion. Climatic Change 64 (1), 41–58.